Wang *Int J Concr Struct Mater* 2023, **17**(1):31
https://doi.org/10.1186/s40069-023-00594-4

International Journal of Concrete Structures and Materials

RESEARCH

Open Access

Experimental Research on Seismic Performance of Masonry-Infilled RC Frames Retrofitted by Using Fabric-Reinforced Cementitious Matrix Under In-Plane Cyclic Loading

Fayu Wang[1,2*]

Abstract

Fabric-reinforced cementitious matrix (FRCM) composites, also known as textile-reinforced mortars (TRMs), represent a new advancement in structural repair and reinforcement technology. Aiming to improve the energy efficiency and seismic performance of existing buildings, this research focused on the development of an FRCM system in combination with phase change materials (PCMs) and extruded polystyrene sheets (XPS) to achieve adequate mechanical and thermal properties for reinforced concrete (RC) and masonry structures. Accordingly, the in-plane behaviour of five FRCM-strengthened RC frames with hollow-brick wall infill was tested under cyclic loading to investigate the improvement in earthquake resistance. The system was comprehensively evaluated by calculating hysteresis curves; comparing the lateral stiffness, ductility, and energy dissipation capacity; measuring the deformations of the specimens; and analysing the failure modes mechanically. Finally, it was proved that this novel integrated approach could significantly enhance the mechanical and seismic performance of masonry-infilled RC frames.

Keywords Seismic performance, In-plane behaviour, Fabric-reinforced cementitious matrix, Phase change materials, Thermal insulation, RC frames, Masonry walls, Structural deformation, Failure mode analysis

1 Introduction

Fabric-reinforced cementitious matrix (FRCM) composites comprising an inorganic matrix of fabrics and cement-based mortar are extensively used in the retrofitting of existing reinforced concrete (RC) buildings. This system is generally known as textile-reinforced mortar (TRM) and has been applied to various substrates for the structural reinforcement of RC structures. The enhanced components can also be referred to as textile-reinforced concrete (TRC) and TRC-strengthened masonry.

Seismic retrofitting techniques for RC structures can be generally classified into local and global methods. Local methods focus on improving the performance of specific structural components and characteristically involve strengthening column–beam connections, sheathing of columns and beams, or strengthening using advanced materials such as fibre-reinforced polymers (FRP) and TRM, in addition to traditional RC jacketing.

Journal information: ISSN 1976-0485 / eISSN 2234-1315

*Correspondence:
Fayu Wang
Fayu_Wang@outlook.com
[1] Beijing Key Laboratory of Earthquake Engineering and Structural Retrofit, Beijing University of Technology, Earthquake Engineering Building, No. 100 Ping Le Yuan, Chaoyang District, Beijing 100124, China
[2] Department of Civil Engineering and Geomatics, Faculty of Engineering and Technology, Cyprus University of Technology, No. 30 Archiepiskopou Kyprianou Str, 50329, 3036 Limassol, Cyprus

These methods are used for the rehabilitation of structures, as they may occasionally require the demolition and reconstruction of the structural members, making them expensive. Meanwhile, global methods focus on the structural level, with all measures aimed at improving the overall behaviour of the structure. The most conventional methods in this category include constructing shear walls, using steel cross-bracing, isolating the base, and strengthening infill masonry.

Among these techniques, strengthening the infill walls may be the least invasive alternative. The most commonly used techniques include sheathing with steel straps, applying a thin layer of concrete to the bricks, attaching pre-fabricated concrete panels to walls with dowels, and gluing steel plates or FRP sheets to walls. An improved extension of gluing can be considered as an application of the TRM technique, as it overcomes the disadvantages of similar methods, such as fire resistance, extra weight, and durability, and enhances material bonding and compatibility (Abu Obaida et al., 2021; Alrshoudi, 2021; Al-Salloum et al., 2011; 2009; Cerniauskas et al., 2020; Papanicolaou et al., 2006, 2007; Raoof & Bournas, 2017a, 2017b; Raoof et al., 2017; Tetta et al., 2015). The technique is based on combining textiles with mortar, which is then applied to brick walls in layers. The textile comprises a yarn-made grid of filament fibres, primarily glass, carbon, aramid, basalt, and p-phenylene benzobisoxazole (PBO).

Currently, a large part of the ageing building stock worldwide needs to be significantly modernised because it has exceeded its service life and/or no longer meets the current mandatory safety and energy standards. Therefore, there is a need to develop technologies and processes to retrofit this building stock in terms of safety and energy, which is challenging. From the perspective of sustainability, the focus should be on developing an integrated structural and energy design methodology for new buildings, which would be preferable over individual measures.

However, for existing buildings, particularly those that have reached a certain age, the problem of seismic and energy inefficiency is paramount, and a similar conceptual approach is required to achieve improvements on both fronts. Recently, it has been shown that such independent retrofit measures should be integrated to enhance overall performance. Attempts to combine seismic efficiency with the environmental benefits of mitigating damage and/or demolition caused by earthquakes have been reported. Subsequently, a multidisciplinary approach has been used to improve building performance, with equal attention paid to seismic and energy efficiencies. To this end, the latest development has proposed a specific novel FRCM system that functions as a single unit and has been used to strengthen masonry walls that were subsequently subjected to out-of-plane cyclic loading under different building configurations (Karlos et al., 2020; Papanicolaou et al., 2007; Triantafillou et al., 2017).

Meanwhile, a local retrofit method involves using FRCM composites on the diagonal bands to target reinforcement against diagonal extrusion, which can damage the infill wall due to frame deformation. Therefore, a total of nine single-storey, one-bay test frames were subjected to quasi-static cyclic in-plane loading history (Ismail et al., 2018). The results of the force–displacement hysteresis curves showed that the RC frame filled with masonry required a larger load than the bare frame to deform to the same lateral displacement, while the specimen reinforced with FRCM was able to displace less under the same load. The hysteretic behaviour of the whole wall reinforcement method was found to be better than the local method. This also shows that FRCM retrofitting techniques can be tailored to specific needs, and local and global methods offer different approaches to improving the performance of the structure.

The modern method of masonry reinforcement has benefited greatly from the application and development of Engineered Cementitious Composite (ECC). This cement-based composite material contains discontinuous short polymeric fibres such as polyethylene (PE), polyvinyl alcohol (PVA), and polyester fibres, which exhibit strain-hardening behaviour and high ductility based on its micromechanics (Singh & Munjal, 2020). ECC is also referred to as ductile fibres reinforced composite (DFRCC) due to its high ductile properties after the first crack. Adding polymeric fibres into the mortar of FRCM can improve the performance of retrofitting masonry walls as well. By incorporating these fibres, the FRCM overlay can be expected that a similar effect to ECC can be achieved, resulting in enhanced ductility and strain-hardening behaviour. This approach offers a promising solution for improving the seismic performance and durability of masonry structures.

Overall, this research focused on the development of a new FRCM system to achieve adequate physical, mechanical, and thermal properties for reinforced concrete and masonry buildings. The previous studies on material properties of FRCM has been completed. The research on suitable PCMs for the FRCM system have been carried out by the University of Cyprus (Illampas et al., 2021), which has determined the selection of PCM materials for energy upgrading. Additionally, the author (Wang et al., 2021) concluded that adding XPS plates for thermal insulation performance also can further enhance the stiffness of FRCM overlays by bonding function. The in-plane performance tests are presented in this paper, in order to provide valuable insights into the physical and

mechanical properties of this novel FRCM system. And the results can inform further development and refinement of this innovative retrofitting method.

2 Test Setup

2.1 Specimen Design

The seismic behaviour of five specimens of hollow brick masonry walls infilled with RC frames (strengthened by FRCM) was investigated to determine their in-plane behaviour. These specimens were composed of the same materials used in previous studies by the author and were tested at the Large Structures Laboratory of Cyprus University of Technology, as depicted in Fig. 1.

The RC frames were constructed in accordance with the European code, using C30 cement. All rebars were securely bound by fine iron wires. The base composed of three parts, each of which was reinforced with encrypted stirrups to ensure its rigidity and stability. Each column had a cross-section of 400 mm × 200 mm and was rigidly connected to its independent foundation. The middle part of the foundation was fixed to the laboratory floor using steel tendons, which served as a permanent base for all five tests. Subsequently, the other two tendons were horizontally connected to the two column foundations to achieve stability of the overall foundation, equivalent to a size of 4000 × 1300 × 400 mm. This design saved materials and replacement time, without compromising the experiment. The rebars reserved on the top of the columns were then bound to the beam and loading slab, and they were poured to form a single-unit. This realised rigid connection of the beam–column joints and allowed for the transfer of load to the entire frame, using the slab as the medium.

Afterwards, the two fixtures were lifted onto both sides of the loading slab, and two tendons were passed through them and the slab, and then connected to the corresponding actuators. Each tendon that went through the slab, fixtures, and the foundation was tightened with a prestress of 350 kN. For these experiments, only the laboratory floor and a reaction wall made of high-strength concrete were used as supports. No additional reaction frame was required due to the symmetrical design of the specimen and the output of 930-mm-long steel fixtures clamped on both sides of the loading slab.

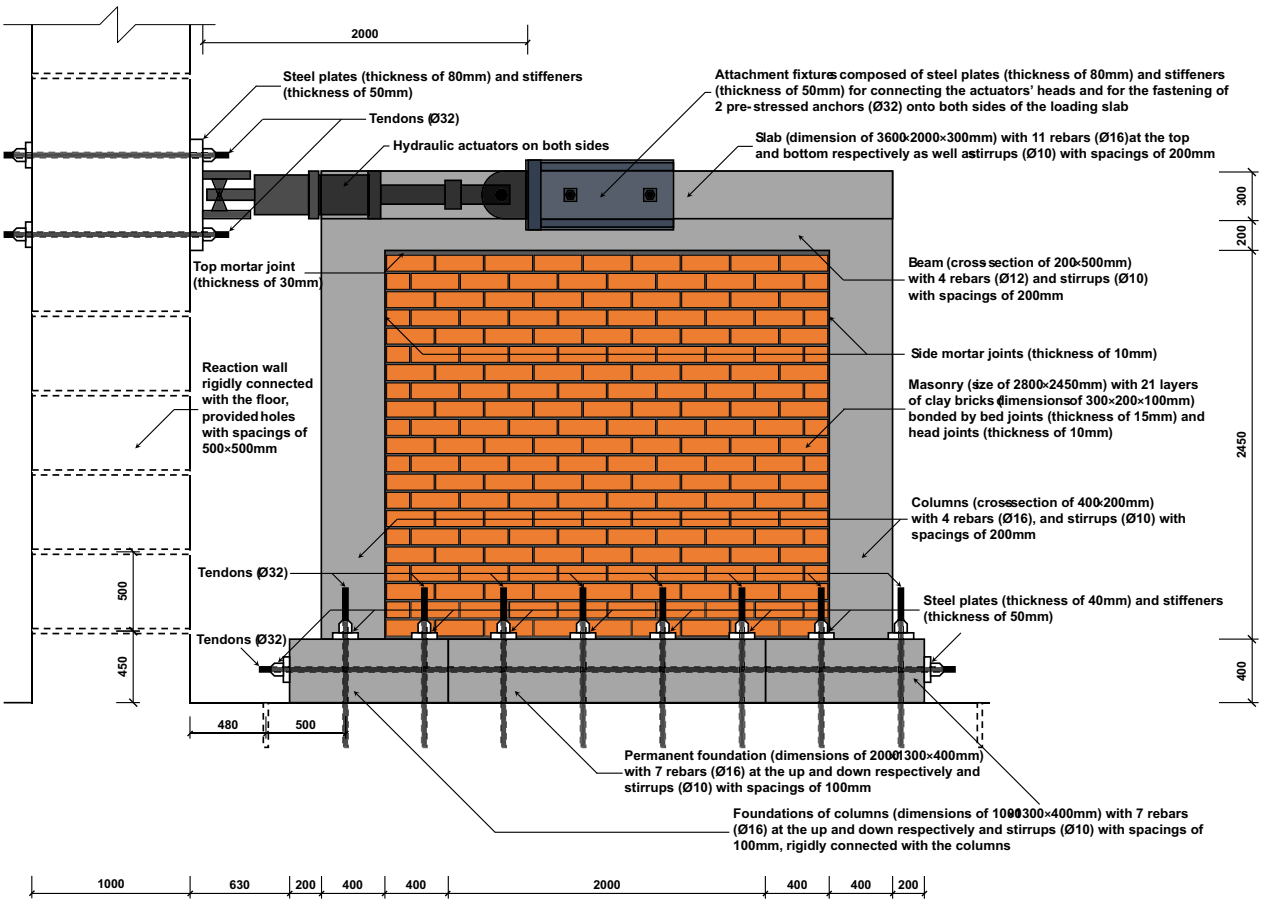

Fig. 1 Details of the test setup (all dimensions are in mm)

The specimens were loaded simultaneously using two hydraulic actuators to prevent horizontal twisting and out-of-plane displacement. Meanwhile, the weight of the slab, the tensile strength of the columns, and connection stiffness of the joints acted as constraints in the vertical direction. This design was intended to simulate a real scenario, as no vertical reaction frame was added to completely restrict the degrees of freedom in the vertical direction.

The concrete covers of all RC components were designed to be 25 mm thick, based on the distance from the outermost side of the reinforcements to the edge of the cross-section. After the completion of the RC frame, each masonry infill wall was constructed using 300×200×100 mm hollow bricks on the 7th day. The bricks were bonded with 20 mm-thick bed joints and 15-mm-thick head joints using staggered joint construction. Enhancement layers were then added, as shown in Fig. 2.

The design of the five test specimens is as follows: Specimen No. 1 consisted of only the hollow brick masonry wall-infilled RC frame. Specimen No. 2 included a thin mortar layer for bonding the XPS layer, as well as one overlayer of FRCM applied to the outside for comparison with the control sample. Specimen No. 3 has two layers of FRCM composite added to the inside and outside of the XPS layer. The inner layer of FRCM was directly bonded to the wall, which was expected to provide better reinforcement than Specimen No. 2. Specimen No. 4 included only one layer of FRCM mixed with PCMs into the mortar matrix, intended to replace the XPS layer for thermal purposes. Finally, Specimen No. 5 was similar to No. 3, but with the application of PCMs to the outer FRCM layer to achieve better thermal insulation efficiency.

The thermal insulation layer comprised 80-mm-thick XPS plates, measuring 600 mm in height, with two different widths of 800 mm and 1600 mm, staggered from bottom to top. Plastic masonry fasteners (PMF) were used to secure each plate, spaced 400 mm apart along the horizontal joints between each level. Additionally, Tsirco thermostatic adhesive material was applied using a notched trowel on both sides of the XPS plates for bonding.

The FRCM layer was developed using SikaWrap-350 alkali-resistant (AR) styrene-butadiene rubber (SBR)-coated glass fibre fabric, buried inside a 10-mm-thick matrix made of Tsirco-Poly-122 cement-based fibre-reinforced polymeric repair mortar (with/without 20% PCM). The SBR coating provided excellent alkaline resistance of the fibres and improved abrasion resistance and heat-ageing properties. The SikaWrap®-350-G-Grid had two orthogonal glass fibre bunches of unequal quantity and spacing. The vertical bundles (weft yarns) weighed 145 g/m^2, spaced 14.2 mm apart and woven using horizontal cords (warp yarns) with a weight of 135 g/m^2, spaced 18.1 mm apart. This commercial mesh was sold in rolls, and the width of each roll was 1000 mm. Thus, each layer of FRCM was arranged horizontally by three tiers

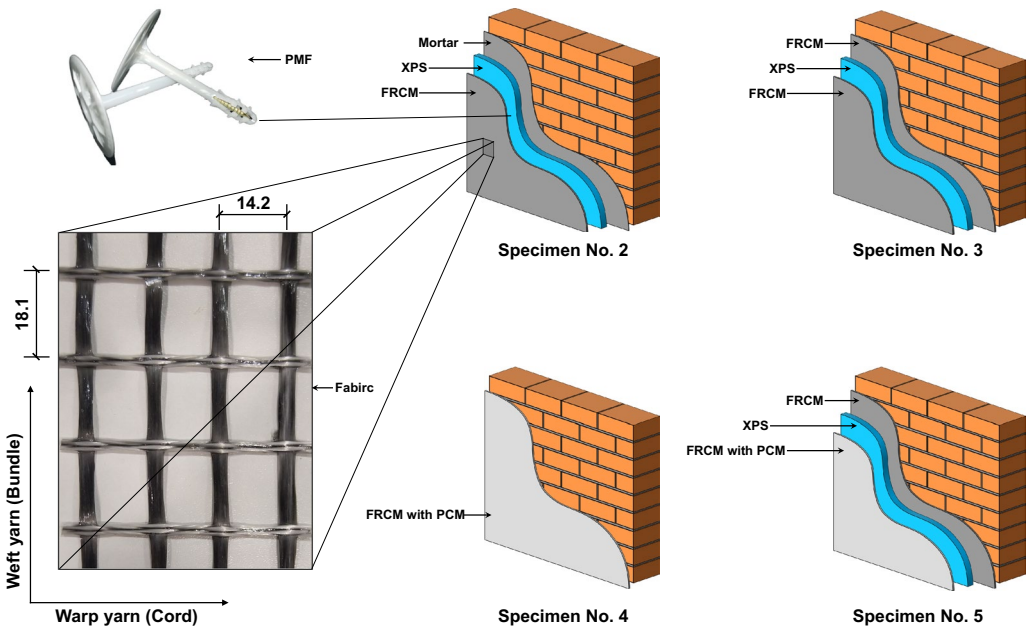

Fig. 2 Details of the overlays (all dimensions are in mm)

of the mesh from the bottom to the top, and the overlap between tiers was 17.5 mm.

The Tsirco-Poly-122 commercial mortar, which was previously tested, was produced by Tsircon® Co., Ltd. In addition to cement, fine aggregates (sand), and polymeric admixtures, this mortar also contains a viscosity modifying agent and short polypropylene fibres. Its durable abrasion and excellent resistance to water, oil, and non-aggressive chemicals improved the protection of internal materials, which enhanced the durability of structures. The most obvious advantages are that fast hardening could be helpful for vertical wall construction, and the strong permeability and high adhesion lead to improved bond properties.

The microencapsulated paraffin Nextek-37D PCM with very high-temperature stability, commercialised by Microtek Laboratories® Inc., was in the form of a white dry powder with a mean particle size of 15–30 μm. It was added to the matrix mortar at 20% by weight for Specimen No. 4 and the outer FRCM layer of Specimen No. 5.

All enhancement overlays were performed on the 9th day after the completion of the frame. Except for Specimen No. 1, which was the control group, all the other specimens were manufactured in 10 days. The installation of the measurement devices and experimental tests were carried out the following day.

2.2 Test Arrangement and Loading Procedures

Fig. 3 shows the details of the instrumentation in the front view of the specimens. Two groups of crossed drawn wires were fixed on the core area of the masonry wall and on the frame to measure diagonal deformation. In addition, two sets of potentiometers connected end-to-end using steel wires were installed vertically at a distance of 100 mm from the outside of the columns to measure elongation. Moreover, pieces of equipment were used to measure the gap between the masonry and the frame after debonding. Near the inner sides of the two columns, two more groups of potentiometers were installed horizontally between the columns and the wall at heights of 300 mm and 2100 mm from the foundation, respectively. Three additional groups of linear variable differential transducers (LVDTs) were installed at heights of 300 mm, 1200 mm, and 2100 mm on the backside of each specimen. Seven horizontal lines were marked within 300 mm with 50-mm gaps in the middle of the junctions between the masonry wall and columns.

The horizontal pulling force exerted by the actuators to the left was considered the positive direction in this test. All the specimens were loaded in the horizontal direction at a constant speed of 0.4 mm/s until failure using displacement control. The shift amounts were designed to be 3, 10, 15, 25, 40, 55, 65, and 80 mm in both the positive and negative directions, as shown in Fig. 4.

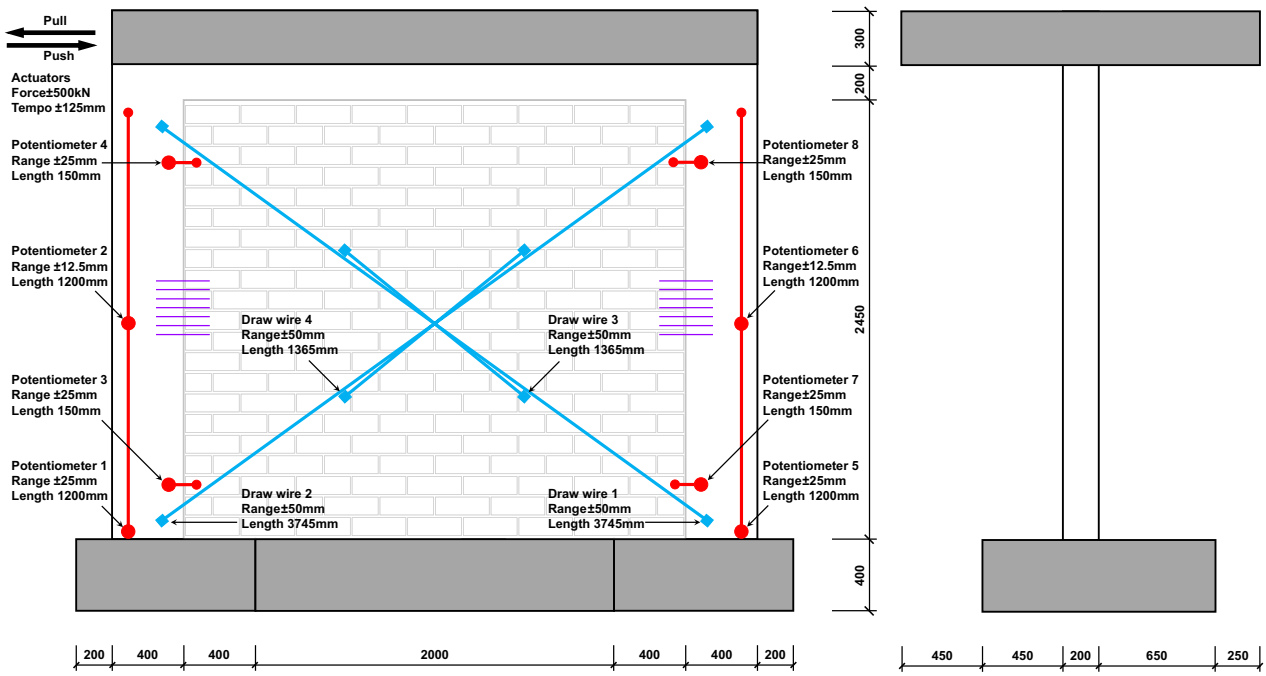

Fig. 3 Details of the instrumentation (all dimensions are in mm)

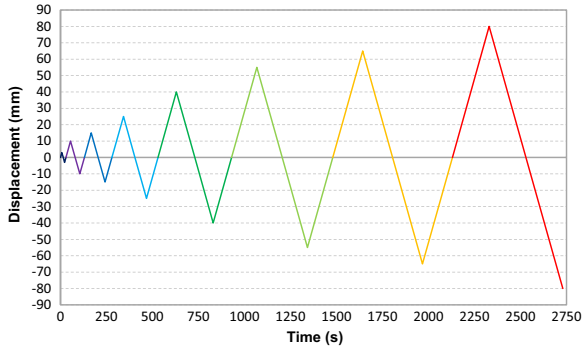

Fig. 4 Loading procedure

Finally, the whitewashed specimens were recorded using a digital camera to observe the details of crack development. A photograph of the test setup is shown in Fig. 5.

3 Failure Mode Analysis

3.1 Observations of Damage

Three cameras were used to record the complete process of each experiment. During the entire loading process, neither the loading slabs nor the foundations were significantly deformed, and all failures occurred in the test areas. The stiffnesses of the beam and the foundation were sufficiently large due to overall reinforcement and pouring of the beam with the slab, the deformation of all frames was primarily realised by the bending and stretching of the column, and the beam–column joints were oblique shear failures at the end.

In the test of Specimen No. 1, which was not reinforced by FRCM, many fine horizontal cracks distributed over the full height of the sides of the columns were observed. The remaining specimens exhibited tensile and bending failures of the FRCM sheathing overlays at the tops of the columns to varying degrees. Debonding between the enhancement layers and RC frames also partly occurred from the front surfaces to the side surfaces of all the columns. At the beam–column joints, the FRCM layers were also sheared obliquely with the frames, and Specimens No. 3 and No. 5 exhibited fibre rupture of the fabric and fragmentation of the matrix.

The failure of the infill walls represented different forms. All specimens suffered brick crushing at the corners at different levels. Among them, the control group was the most serious, and the level of damage decreased as the FRCM layers increased. However, the development of cracks was the opposite. The less crushed the wall, the more uniform the shear stress distribution, and the cracks were fine, but the distribution range was much wider. Because hollow bricks were used in this experiment, many partially crushed bricks were exposed on the on the wall surfaces. Meanwhile, some completely crushed bricks would also have some fragments remaining on the wall, but they would have lost almost all the bearing capacity.

The complete details of each specimen test area after testing were obtained from the videos. The images were processed with increased sharpening, higher contrast, and lower colour saturation so that the cracks appeared clearly. Photographs and corresponding drawings are shown in Fig. 6.

This experimental study revealed varying degrees of shear sliding failure, shear diagonal failure, and corner crushing failure of the masonry as specified. However, none of these specimens was destroyed by a single mode. To further study the causes of different failure types, it is necessary to combine the deformation of the specimens and the specific mechanical mechanism to conduct failure mode analysis.

3.2 Diagonal Extrusion of Masonry-Infilled RC Frame

Masonry infill walls commonly fail due to brick crushing in the corners and step-type cracks between the bricks and mortar joints, which are typical baroclinic failures caused by diagonal extrusion of the RC frames and the insufficient compressive and shear strengths of the masonry. To investigate this factor, Fig. 7 compares the changes enhanced by different FRCM layers using measured data from two groups of draw wires set on all specimens. It should be noted that some test failures occurred during the tests, which were corrected to present the original image. For example, draw wires were hit by broken bricks, causing many huge fluctuations lasting 0.2–0.6 s. These invalid data were precisely eliminated, and parts of the data exceeding the test range or dislocations due to the draw wires being pressed by broken bricks were reset by adding fixed correction values. Therefore, the original data of this figure were preserved to the greatest extent, but there may be a correction error of no more than 1 mm near the peak of the latter half of the tests. The corresponding data of draw wires were assigned different colours for clarity.

In the line charts, it can be observed that the diagonal deformation displacements of the central masonry and peripheral RC frame are not directly proportional to the measured distances, indicating only a positive correlation. The data tested from the same group of draw wires show substantial symmetry on the horizontal axis.

The diagonal deformations of the walls located in the central regions of Specimen No. 1 and No. 2 were extremely small. The data of the crossed draw wires were axisymmetric to each other in the first five cycles. However, the subsequent positive correlation occurred

Fig. 5 Photo of the test setup (Specimen No. 5)

because of the horizontal cracks that developed at the middle height of the walls. The same displacements were the gaps caused by cracks. However, the masonry of Specimen No. 4 did not exhibit horizontal cracks after being crushed diagonally, so the diagonal displacements of the central region consistently approached zero. Specimens No. 3 and No. 5, which were strengthened by double-layer FRCM, were different. The diagonal displacements of the central masonry were large, which did not indicate that the stiffness of the walls was low. Instead, this was because the walls protected by two layers of FRCM were not severely crushed, indicating that the synergy between the infill walls and the RC frames was maintained well. This discovery proves that using the global method of reinforcement by the FRCM system can effectively enhance the overall stiffness of the masonry-infilled RC frame and prevent premature failure of the brick wall.

The diagonal displacements of the RC frames changed with cyclic loading. The data of crossed draw wires were negatively correlated with each other. However, the sum of values of two draw wires in the same group increased due to the tensile deformation of the columns during the later stage of loading. This increase was also observed in elongation measurements of the columns.

3.3 Deformation of RC Frame

In this study, hydraulic actuators were used to apply displacements to the masonry-infilled RC frame. The horizontal loads were then transmitted to the beam and beam–column joints through the loading slab. The bottom base provided support through its high rigidity and the connection between the foundations and the floor. Because the beam was cast integrally with the loading slab, its stiffness was sufficiently high to resist the horizontal shear force, resulting in a lateral displacement with a twist of the entire frame, as well as bending deformation occurring at both ends of the columns. Furthermore, the masonry infill wall acted as a diagonal strut to prevent the deformation of the frame. Therefore, the tension side of the frame was slightly upturned due to the absence of a vertical reaction frame. Two sets of potentiometers near the outsides of both columns were used to measure the changes in the length of the columns as they underwent tensile and flexural deformations, as shown in Fig. 8. The potentiometer at the bottom of the right column of Specimen No. 5 had some measurement faults, and its data image was fixed and corrected by adding 0.6 mm upward.

The graphs illustrate that the top and bottom length changes in each column are almost equal at the beginning. The upper parts change less than the lower parts of both columns and exhibit positive correlations consistently. In other words, the upper parts of the columns are always in tension when the horizontal displacement load is received, and continue moving with the drifted beam. Instead, stretches of the lower parts of the columns on both sides were negatively correlated. When the specimen rotates, the bottom of one column bends by compression, while the bottom of the other column bends by tension. However, all the tested plotlines were essentially above the horizontal axis due to the high compressive strength and stiffness of concrete. Moreover, the peak stretch values in the lower parts of the columns decreased with an increase in the number of reinforced FRCM layers. This is because columns are equivalent to three-sided textile-reinforced concrete members before

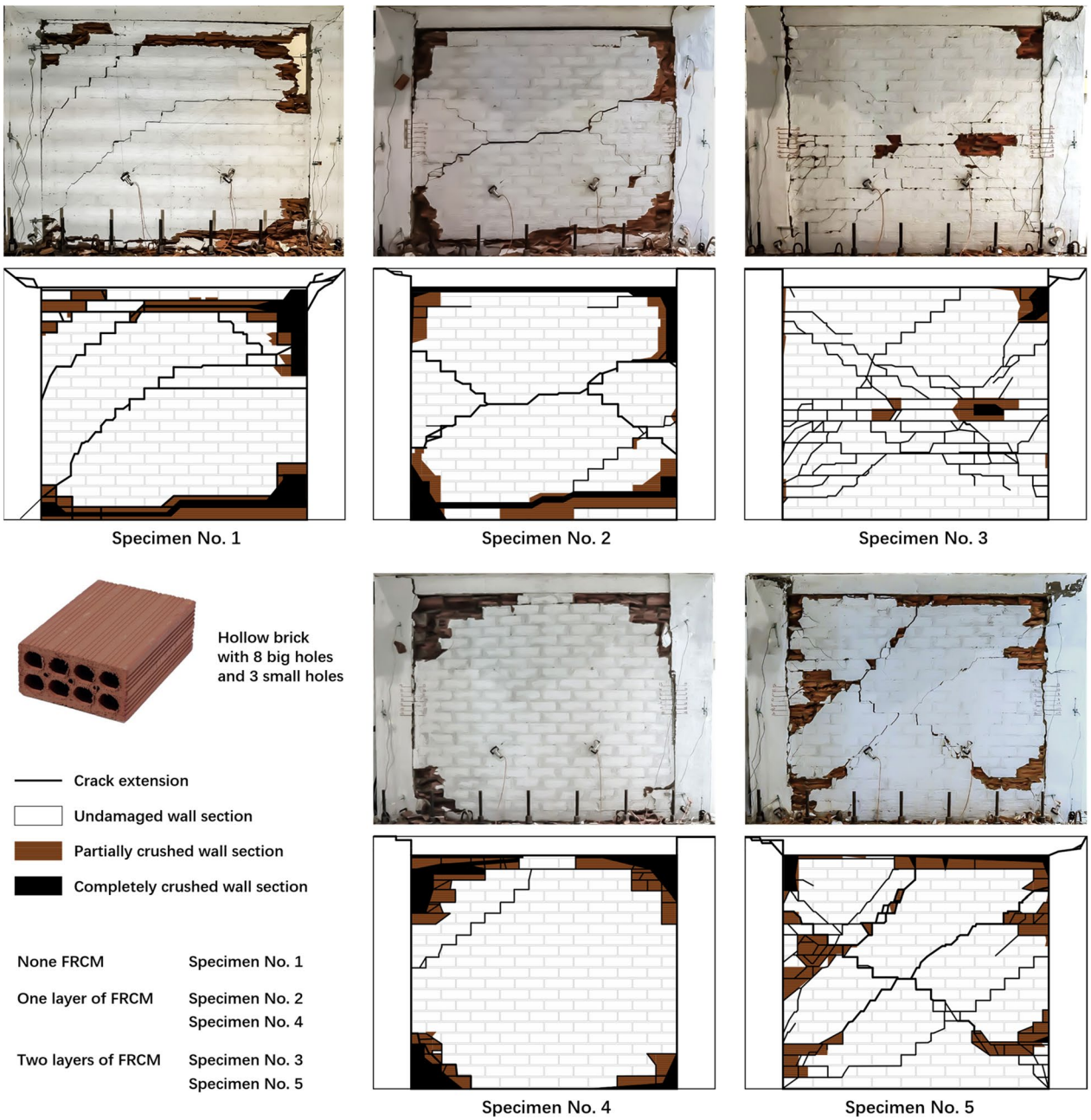

Fig. 6 Failure details of all specimens

the bond failure between the FRCM overlays and the RC frame occurs, reducing the failures by shear and bending. These results indirectly prove that the strength and stiffness in compression, tension, shear, and bending of FRCM-strengthened concrete are enhanced, and the FRCM composite can also effectively enhance both the shear strength and ductility of seismically deficient beam–column joints. This is consistent with the TRC research conclusions of (Al-Salloum et al., 2011; Bournas et al., 2009; Colajanni et al., 2014; Faleschini et al., 2019; Ngo et al., 2020; Shi-ping et al., 2020; Toska et al., 2021; Tomasz Trapko, 2014; T. Trapko & Musial, 2020; Yan et al., 2021; Yin et al., 2017).

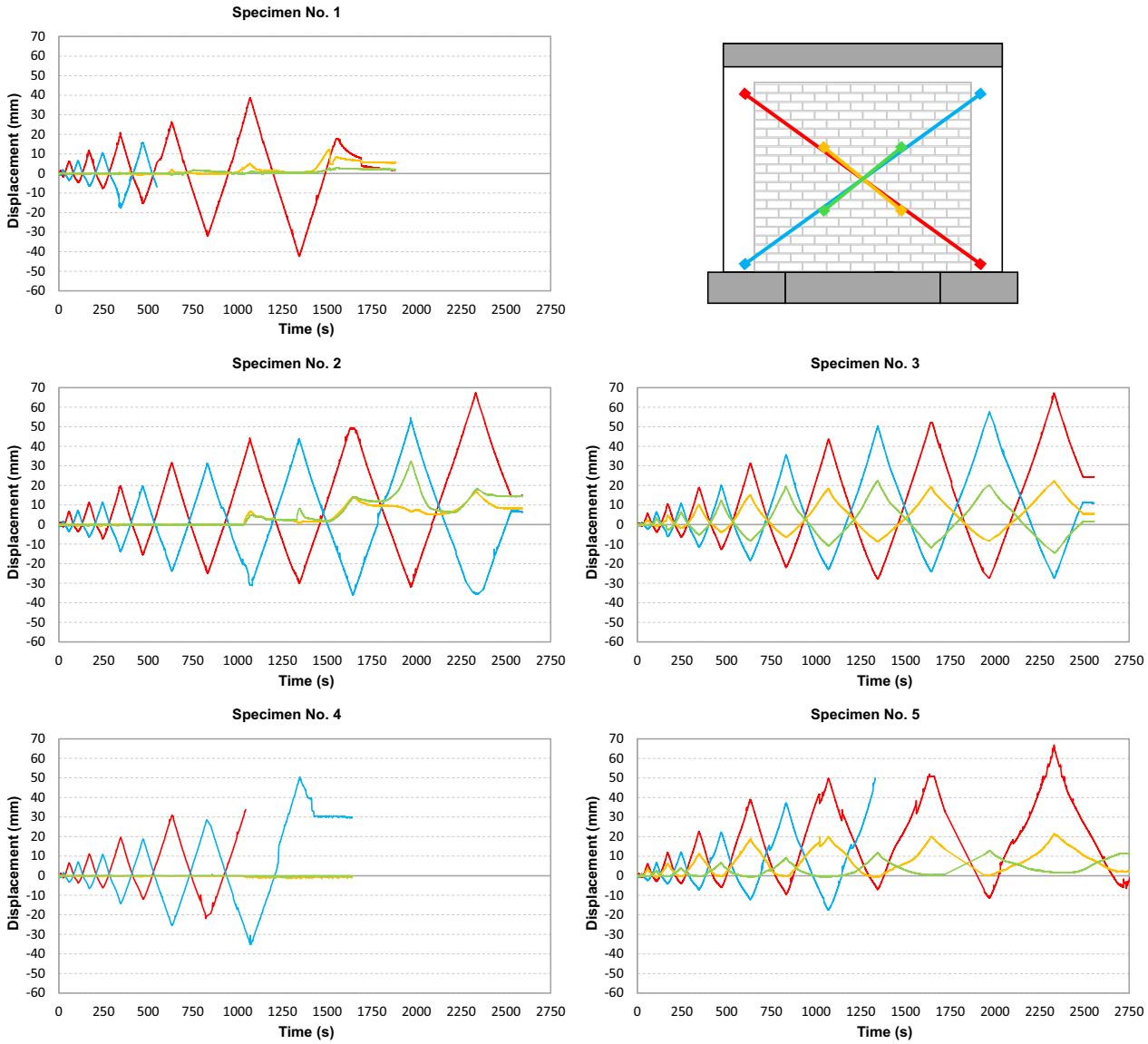

Fig. 7 Measured changing of diagonal distances

3.4 Dislocations and Gaps Between Masonry and RC Frame

The combined effects of load and deformation caused bond failure between the masonry and RC frame interfaces, resulting in gaps and dislocations.

Notably, Specimen No. 2 experienced severe horizontal shear failure at the bottom of the masonry, causing the infill wall slipped horizontally and sink approximately 50 mm after testing. Furthermore, owing to the diagonal crushing failure of the infill wall that occurred in Specimen No. 4, the overall shape of the infill wall was approximately obliquely pressed into a circle, and the masonry rotated counter-clockwise or clockwise with the deformation of the RC frame. Before the masonry suffered from severe crushing failure, the dislocations in the vertical direction between the wall and the columns increased with the loading displacement but decreased with addition of FRCM layers, as observed from the marker lines on the left and right sides of each specimen. Meanwhile, the tested displacements of the upper and lower groups of potentiometers as solid lines, as well as the upper, middle, and lower groups of LVDTs (dotted lines), are shown in Fig. 9, which illustrates the gaps between the masonry and both sides of the columns.

First, additional LVDTs were added to the side of each base, and their displacements were found to be

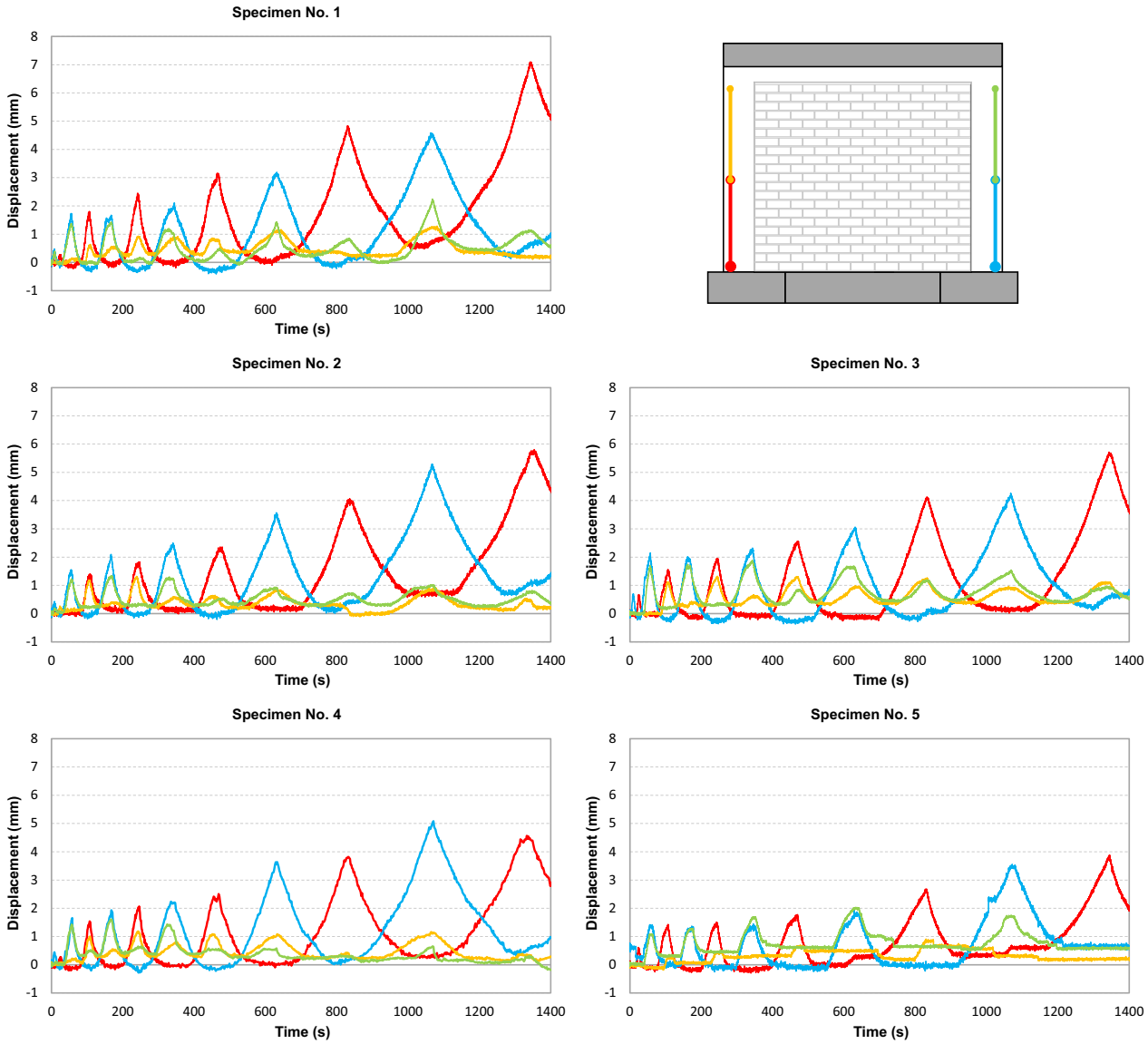

Fig. 8 Measured changes in the length of columns

substantially near the horizontal axis throughout the entire loading process, demonstrating that the overall stability of the prestress-clamped three-part base was sufficient. Second, a negative correlation was observed between the measured displacements of the left and right symmetrical instruments, indicating that when one side between the masonry and column forms an open gap, the other side is squeezed closed. Third, the polylines of the instruments at the same position are coloured the same, but the measured displacements of the LVDTs at the backside of each specimen were slightly smaller than the data of the potentiometers in the front view. This is primarily because the potentiometer can be rotated, allowing the measured data can be used to estimate the vertical displacement component, whereas the LVDT can only measure unidirectional displacement. The platforms appear in the data at the later stage of the test due to being beyond the testable range of the potentiometers.

However, except for the data of Specimen No. 3, only the first 800 s of data for other specimens are shown in the figure because some instruments fell off in the subsequent process owing to the corner crushing failure of the wall, resulting in irregular data, particularly for Specimen No. 1.

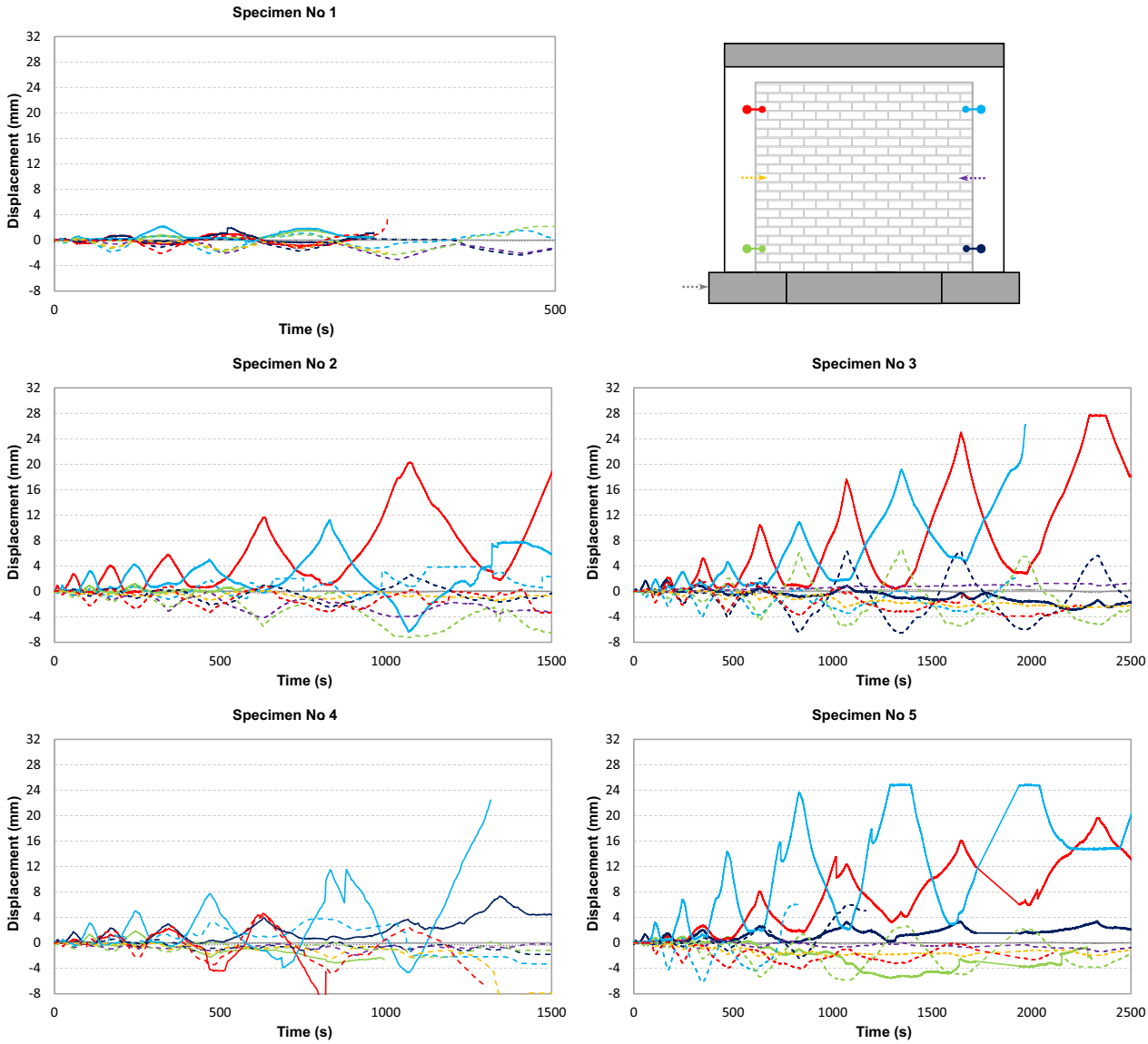

Fig. 9 Measured changes of gaps between masonry and columns

3.5 Mechanical Mechanism of Failure Modes

Diagonal compression tests have been commonly used to study the in-plane behaviour of different types of walls strengthened by the FRCM system. This method is the most direct and easy way to test the improvement in the shear strength and stiffness of the masonry by FRP or FRCM enhancement. However, experimental research on full-scale masonry-infilled RC frames is still necessary. This is because the failure modes of walls are not only limited to diagonal compression, as observed in this research and other experimental studies (Akhoundi et al., 2018; Ismail et al., 2018; Morandi et al., 2018; Ricci et al., 2018; Sagar et al., 2019). Therefore, it is theoretically flawed to study the infilled masonry of RC frames solely through diagonal compression tests on wallettes.

Based on the analysis of the above test results, it was determined that the masonry infill wall in the RC frame, under the effect of horizontal loading, underwent diagonal compression during the initial loading process. As the lateral displacement of the frame increased, the deformation of the concrete member also increased. This was primarily manifested in the tension bending and compression bending at the upper and lower ends of the columns in this experiment. Since the location and degree of deformation are influenced by the strength and stiffness of the reinforced concrete frame,

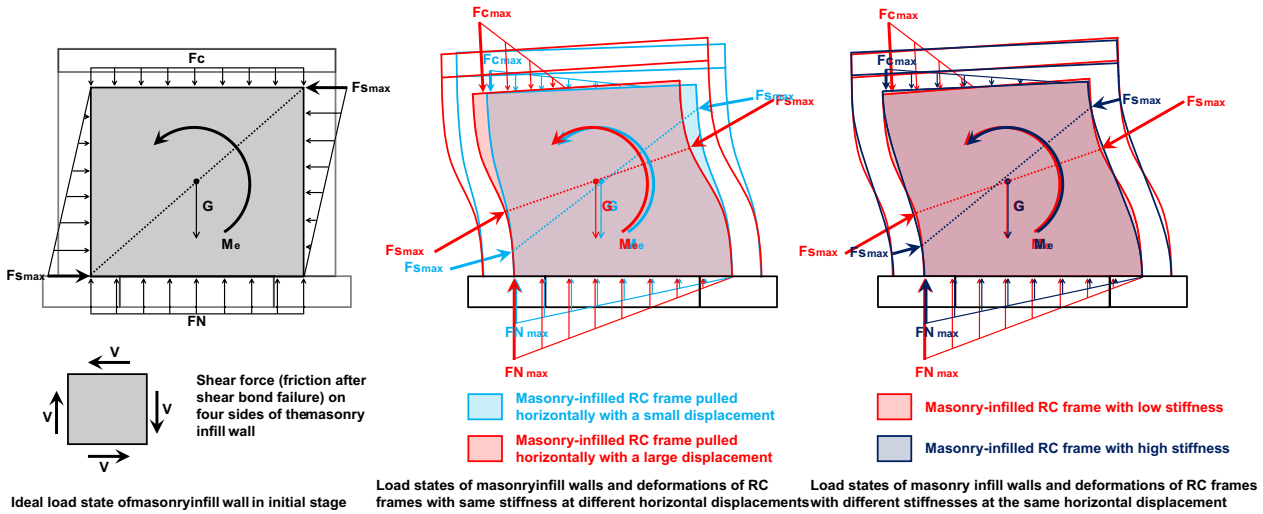

Fig. 10 Load state of masonry infill wall changed by deformation of RC frame

the load state and failure mode of the infill masonry also changed accordingly. The mechanical mechanism of this function is presented in Fig. 10.

During the entire test process, the beam did not deform significantly since it was cast integrally with the loading slab. To simplify the illustration, it is assumed that the stiffness of both the beam and the base is infinite, as both yield and failure occur in the columns. This is typically referred to as the detrimental type of strong beam and weak column in RC structural design.

At the initial loading stage, when the loading slab is displaced in the left direction, the lateral displacement of the masonry-infilled RC frame is small, and the ideal load state of the infill wall is similar to diagonal compression, as shown in the first drawing. In this process, the concrete components do not deform significantly, and their stiffness is not reduced, causing the frame to tend towards a parallelogram. The bottom of the beam creates a small uniform pressure (*Fc*) above the infill wall, and the support force (*FN*) from the base to the bottom of the wall is equal to (*Fc*) and the gravity (*G*) of the wall.

The horizontal shear force on the frame also causes the columns to squeeze against the wall, and the extrusion forces (*Fs*) of the infill wall are distributed on the interfaces of both sides. The maxima of the two forces at the lower-left corner and upper-right corner also provide a moment (*Me*) of a couple to the wall, resulting in a counter-clockwise rotation. At the same time, shear bond failure occurs in the masonry-frame interfaces, particularly between the underside of the beam and the top of the infill wall. The shear stress track experienced by the wall is diagonal, resulting in shear failure of the mortar joints and shear bond failure of the interfaces between the mortar and bricks, depending on which shear strength is smaller. The cracks extend in step-type pattern through the diagonals to the centre of the infill wall until docking. The bricks at the corners may be crushed if their compressive or shear strengths are insufficient, and Specimen No. 1 is most damaged in this stage.

However, with an increase in horizontal displacement, two types of RC frame deformations occur, as depicted in the second drawing. In the first type, due to the absence of a vertical reaction frame, the lower-left corner of the infill wall acts as the fulcrum of the diagonal brace, which lifts the upper-right corner of the frame. The entire frame inclines, leads to the deflection pressure from the beam bottom to the wall top, further exacerbating the crushing of the masonry corners. Ultimately, the masonry wall without four crushed corners rotates in-plane within the RC frame, as seen in Specimen No. 4.

In the second type, flexural yielding creates two bending points equivalent to plastic hinges at both ends of the columns owing to. As the degree of yield increased, the bending points moved from both ends of the columns. The convex points where the columns bend into the frame cause stress concentration and migration of the shear strain track of the wall. This is the primary reason why the wall cracks that occur later are not diagonal but at the middle height of the wall, as in the failure mode of Specimen No. 2 in this study.

Finally, FRCM-strengthening can improve the stiffness and ductility of concrete members, as mentioned before. The third drawing expresses the modification deformation of different stiff RC frames with the same amount of side shift. The increased stiffness results in

a smaller elongation of the columns and a more negligible deflection of the frame. Thus, the bending angle of each concrete member is reduced, and the pressure on the wall top becomes more uniform. Meanwhile, the stiffness ratio of the beam to column and the ratio of the connection stiffness of the beam–column joints to the bending stiffness of the columns are reduced. As a result, the position of the column bend to decrease, thereby making the maximum squeeze force (*Fs max*) created by the columns to the wall closer to the ends of the columns, and the inner sides of the columns become straighter.

Because the horizontal shear strain of the mortar joint originates from the relative displacement of the upper and lower bricks, the interlaminar shear force generated by the straighter column on the wall is more evenly distributed, effectively avoiding the stress concentration effect. Although cracks appeared in the mortar joints of almost all layers, the damage to the masonry is not concentrated. Therefore, the failure modes of Specimen Nos. 3 and 5 were caused by the above reasons.

Overall, the principle of the global upgrading method of the FRCM system to improve the in-plane performance of a masonry-infilled RC frame was verified.

4 Seismic Performance Evaluation

4.1 In-Plane Load–Displacement Response

Generally, the seismic performance of a structure is evaluated by the lateral stiffness, ductility, and the energy dissipation capacity, as mentioned by Su et al., 2017). The load–displacement responses of all specimens, which were measured using two actuators, are presented as hysteresis curves in Fig. 11. The data of different loading cycles are in varying colours, ranging from cool to warm.

The hysteresis curves reveal that there are many fluctuations in the data between the second and sixth cycles, which are attributed to the destruction of the infill walls and the steps of shear bond failure between the infilled frames and FRCM overlayers. Although the bearing capacity of Specimen No. 5 was not as strong as that of Specimen No. 3 in the early and late stages, it endured an additional half-loop, and their data graphs were similar. However, Specimen No. 2, which was also reinforced with one layer of FRCM, performed better than Specimen No. 4 due to the use of XPS, which enhances the tensile strength and overall stiffness of the entire overlay through the chemical bonding of the mortar and interlocking of the PMFs.

Overall, the FRCM system demonstrated an impressive enhancement of in-plane performance for masonry-infilled RC frame retrofitting. The load required to achieve the same displacement increased with the number of strengthened FRCM layers in the specimens, and they are able to withstand more loading cycles before failure.

4.2 Lateral Secant Stiffness

Stiffness is a crucial index for evaluating the ability of RC structures to resist deformation, and a global elastic analysis of RC elements is effectively performed using it. Since this research was conducted at a constant speed using a displacement-controlled strategy, the peak load of each cycle was essentially at the maximum displacement. Therefore, the average stiffness (K_i) was used to compare the FRCM layers calculated using the positive or negative values of the maximum horizontal displacement ($\Delta_{i,\,max}$) and the corresponding lateral force ($V_{i,\,max}$). The data and results are presented in Table 1 and Fig. 12.

It can be observed from the changes in the line graphs that the FRCM significantly enhanced the stiffness of the specimens during the initial stages. The improvement by the FRCM is related to the number of layers and strength of the matrix, which are positively correlated because the strength of the mortar after adding 20% PCM is slightly lower than that of the original mortar matrix. These findings also verify the previous conclusions of (Wang et al., 2021), which showed that adding additional layers of fabric and increasing the strength of the mortar can enhance the overall stiffness of the matrix to strengthen the substrate, achieved through the matrix-to-substrate bond mechanisms between the overlays and the infilled frames.

However, due to the destruction of the wall, debonding of the overlay, and rupturing of the fibre, the overall stiffness is significantly reduced in the first two cycles and is almost identical to that of the control group in the later period.

4.3 Lateral Displacement Ductility

Ductility is an essential property of RC structures that measures their ability to deform without significant reduction in their resistance strength. In the conducted tests, no apparent yielding under uniform loading was observed, and the hysteresis curves showed plateaus whenever the drift was near the maximum displacement. The ductility of each half-cycle was calculated by the ratio (μ) of the maximum displacement ($\Delta_{i,\,max}$) to the corresponding displacement (Δ_y) at 0.85 times the maximum lateral force, as depicted in Fig. 13.

Although the ductility values for the tested specimens were irregular, the specimens reinforced with FRCM demonstrated significantly higher ductility compared to the control group in the first two cycles of loading. Additionally, the peak values of Specimens No. 3 and No. 5 in the fourth half-cycle were greater than those of the other specimens. These results suggest that the ductility of the

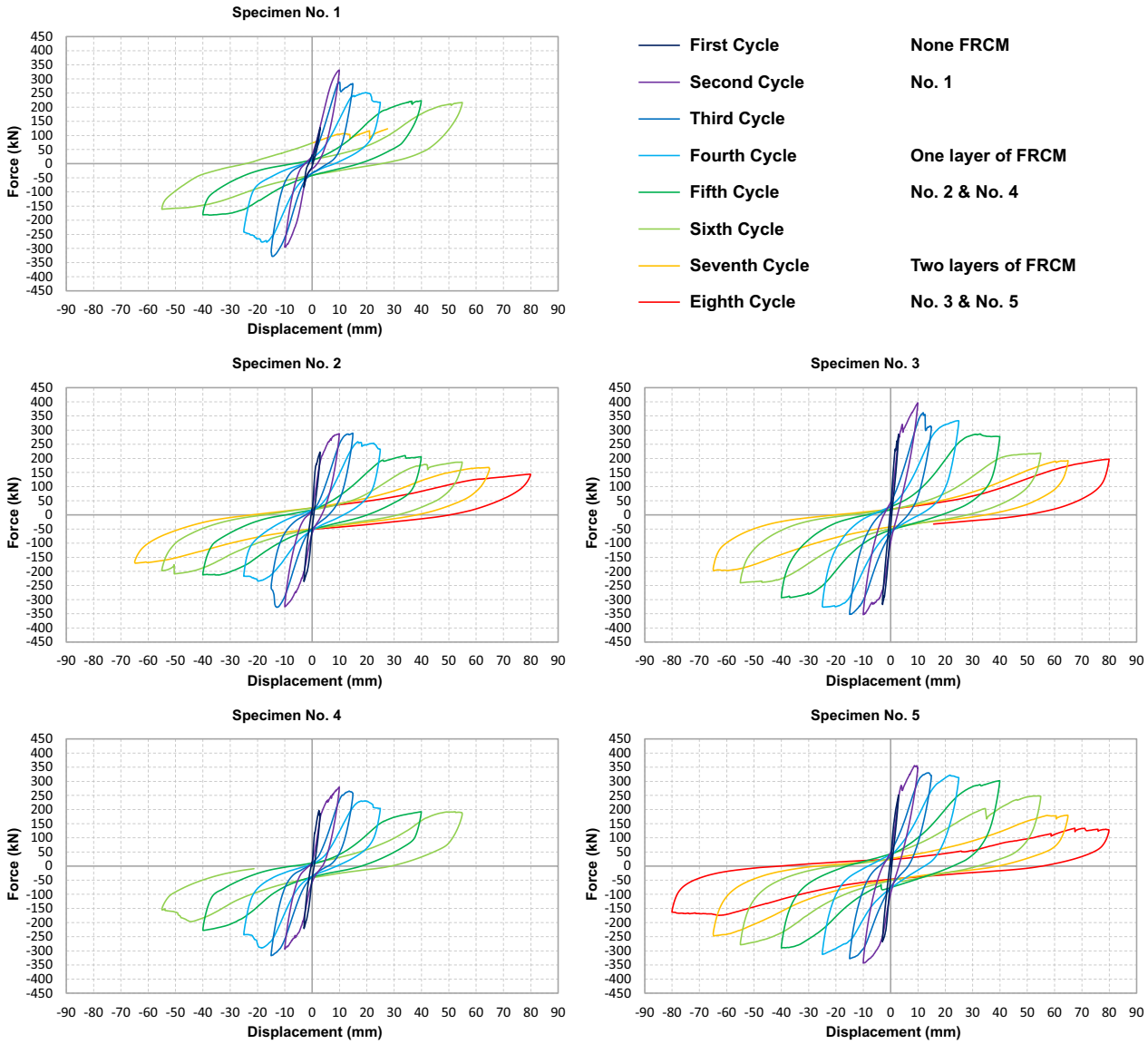

Fig. 11 Hysteresis curves of all specimens

infilled frames is improved before shear bond failure occurs in the FRCM overlays, which is consistent with the diagonal distance measurements.

4.4 Energy Dissipation Capacity

The energy dissipation capacity of RC structures is a measure of their ability to absorb earthquake energy caused by ground vibrations and is represented by the area enclosed by the hysteretic curve. The dissipated hysteretic energy (E_i) of each half-cycle was calculated using the integral method in the mathematical calculation software, OriginPro®. The corresponding coefficients are listed in Table 2. The total energy dissipated (E_t) is shown in Fig. 14. The equivalent viscous damping coefficient (v_{eq}) was calculated using the following equation:

$$v_{eq} = \frac{E_i}{2\pi \times \Delta_{i,\max} \times V_{i,\max}}, \quad (1)$$

where v_{eq} is the equivalent viscous damping coefficient, E_i is the dissipated hysteretic energy, Δ_i, max is the maximum displacement, $V_{i,max}$ is the maximum shear force.

Except for Specimen No. 4, the total dissipated energy and equivalent coefficients of the in-plane behaviour significantly improved as the number of FRCM layers increased, particularly in the later cycles.

Table 1 Summary of maximum horizontal displacements and corresponding lateral forces

Stage		Specimen no. 1		Specimen no. 2		Specimen no. 3		Specimen no. 4		Specimen no. 5	
		$V_{i,max}$ (kN)	$\Delta_{i,max}$ (mm)	$V_{i,max}$ (kN)	$\Delta_{i,max}$ (mm)	$V_{i,max}$ (kN)	$\Delta_{i,max}$ (mm)	$V_{i,max}$ (kN)	$\Delta_{i,max}$ (mm)	$V_{i,max}$ (kN)	$\Delta_{i,max}$ (mm)
First cycle	P	127.70	2.91	222.41	2.91	285.46	2.91	186.84	2.91	251.43	2.91
	N	− 83.64	− 3.01	− 235.93	− 3.01	− 316.55	− 3.00	− 221.17	− 3.00	− 268.23	− 3.00
Second cycle	P	331.01	9.93	287.61	9.92	396.80	9.93	279.70	9.93	348.71	9.93
	N	− 95.59	− 10.03	− 325.25	− 10.03	− 353.41	− 10.02	− 294.38	− 10.02	− 343.42	− 10.02
Third cycle	P	283.27	14.89	289.21	14.88	312.01	14.90	257.93	14.89	321.07	14.89
	N	− 313.26	− 14.99	− 258.62	− 15.00	− 352.21	− 15.03	− 317.36	− 15.03	− 327.63	− 15.03
Forth cycle	P	217.31	24.92	232.56	24.91	332.08	24.94	204.23	24.93	312.82	24.93
	N	− 241.56	− 25.02	− 217.36	− 25.03	− 324.82	− 25.00	− 243.44	− 25.01	− 312.66	− 25.00
Fifth cycle	P	222.99	39.93	205.76	39.90	276.93	39.94	192.52	39.92	301.90	39.93
	N	− 180.83	− 40.01	− 212.52	− 40.03	− 292.92	− 40.00	− 227.79	− 40.01	− 290.05	− 40.01
Sixth cycle	P	216.56	54.93	187.26	54.88	218.23	54.94	185.16	54.91	247.30	54.92
	N	− 161.26	− 55.00	− 197.54	− 55.04	− 240.43	− 55.03	− 155.06	− 55.00	− 278.23	− 55.00
Seventh cycle	P	–	–	164.35	64.91	192.10	64.93	–	–	179.79	64.89
	N	–	–	− 165.13	− 64.93	− 189.35	− 64.93	–	–	− 237.32	− 64.92
Eighth cycle	P	–	–	144.22	79.91	197.58	79.92	–	–	128.47	79.89
	N	–	–	–	-	–	–	–	–	− 163.11	− 80.02

'*P*' denotes positive direction; '*N*' denotes negative direction

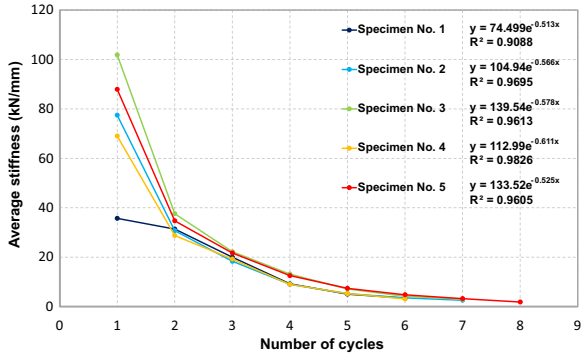

Fig. 12 Average stiffness versus each cycle

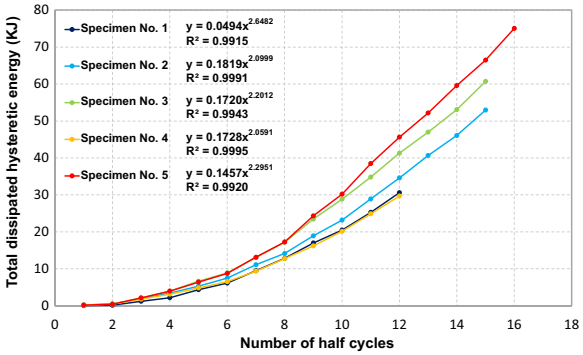

Fig. 14 Total dissipated energy versus each half-cycle

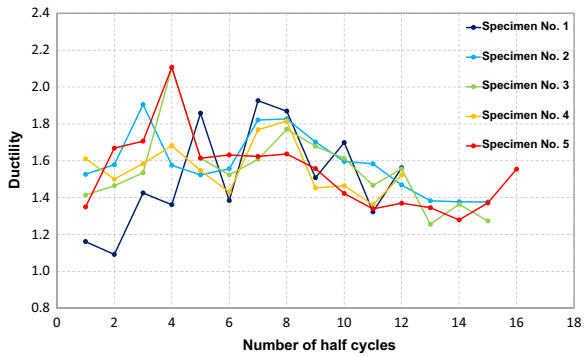

Fig. 13 Ductility versus each half-cycle

5 Conclusions

To summarize, five specimens were subjected to in-plane cyclic loading. The effectiveness of the FRCM system in enhancing masonry-infilled RC frames (in the order of Specimens No. 2 to No. 5) was demonstrated through failure mode analysis and seismic performance evaluation, as presented in Fig. 15. The following conclusions can effectively guide further research:

1. Applying an equivalent uniform load using two actuators through the loading slab can prevent horizontal torsion of the specimen. Deformation of the specimen can be made more realistic by not locking the longitudinal degrees of freedom.

Table 2 Summary of dissipated hysteretic energies and equivalent viscous damping coefficients

No. of half-cycles	Specimen No. 1		Specimen No. 2		Specimen No. 3		Specimen No. 4		Specimen No. 5	
	E_i (KJ)	v_{eq}	E_i (KJ)	v_{eq}	E_i (KJ)	v_{eq}	E_i (KJ)	v_{eq}	E_i (KJ)	v_{eq}
1	0.060	0.026	0.241	0.059	0.218	0.042	0.228	0.067	0.174	0.038
2	0.089	0.056	0.249	0.056	0.230	0.039	0.224	0.054	0.240	0.047
3	1.058	0.051	1.510	0.084	1.666	0.067	1.355	0.078	1.710	0.079
4	0.962	0.052	1.429	0.070	1.857	0.083	1.325	0.071	1.847	0.085
5	2.179	0.082	1.883	0.070	2.675	0.092	1.703	0.071	2.435	0.081
6	1.811	0.061	2.186	0.090	2.244	0.067	1.689	0.056	2.339	0.076
7	3.338	0.098	3.611	0.099	4.166	0.080	2.846	0.089	4.388	0.090
8	3.332	0.088	3.031	0.089	4.120	0.081	3.388	0.089	4.123	0.084
9	4.175	0.075	4.790	0.093	6.293	0.091	3.467	0.072	7.084	0.094
10	3.486	0.077	4.268	0.080	5.390	0.073	3.931	0.069	5.856	0.080
11	4.783	0.064	5.724	0.089	5.962	0.079	4.721	0.074	8.278	0.097
12	5.322	0.095	5.667	0.083	6.468	0.078	4.813	0.090	7.168	0.075
13	–	–	6.078	0.091	5.685	0.073	–	–	6.527	0.089
14	–	–	5.413	0.080	6.098	0.079	–	–	7.429	0.077
15	–	–	6.878	0.095	7.643	0.077	–	–	6.866	0.106
16	–	–	–	–	–	–	–	–	8.599	0.105

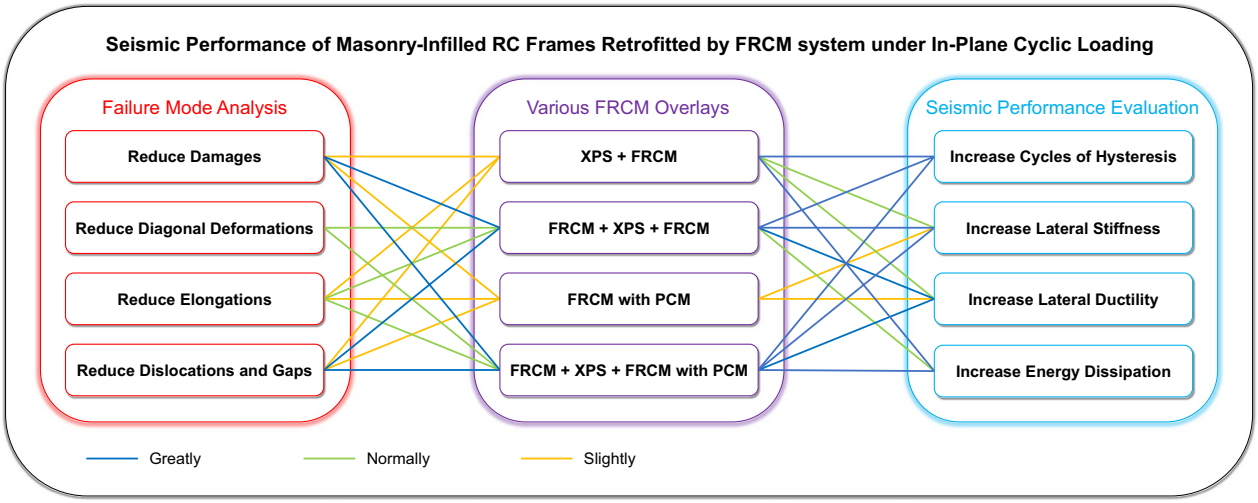

Fig. 15 Research conclusions of failure mode analysis and seismic performance evaluation

2. The prestress-clamped three-part base can save materials and replacement time without affecting experimental results.
3. The bond strength between the FRCM overlay and the wall-infilled frame is directly related to the strength of cement-based mortar, which determines the overall retrofitting effect and seismic performance improvement. This conclusion, combined with previous studies on material properties, is significant for further research.
4. The addition of the FRCM system significantly improves the overall stiffness of the infilled frame, particularly in the first and second cycles of loading. It can also prevent premature failure of the masonry wall.
5. Adding two layers of FRCM further enhances the performance of masonry-infilled frame, enabling it to withstand higher cyclic loading before complete failure. It can improve lateral stiffness, ductility, and energy dissipation capacity, as well as reduce the deformation of the RC frame that changes the load state of the infill masonry.
6. PMFs added to the insulation layer of XPS are equivalent to shear connectors, significantly improving the mechanical interlocking between the FRCM layer and the wall in the early stage of loading, thereby improving the overall stiffness of the frame wall. However, drilling holes in the wall may accelerate crack propagation, and the residual stage may not be significantly affected until the wall is damaged to a large extent and overall fracturing. Therefore, shear connectors should be added carefully and only be sufficient to embed the insulation layer.
7. Placing the FRCM layer on the inner side of the overlay and direct bonding to the wall has a stronger reinforcing effect than placing the FRCM layer on the outer side of the insulation layer, especially for specimens with only one layer of FRCM. Adding two layers of FRCM, one on each side of the reinforcement layer, can serve as a shell to protect the insulation layer, effectively improving the seismic performance and durability of the structure and enabling higher energy efficiency in buildings. This is the ideal retrofitting method used in the current research.

The study elucidated, for the first time, the reinforcing effect of the FRCM system on a masonry-infilled RC frame as well as the mechanical mechanism of each failure mode caused by the change in the load state of the masonry infill wall due to RC frame deformation. The bending position of the RC frame dynamically changes as the amount of side shift increases, and the changing law and scope of this phenomenon are related to the proportional relationship of stiffness of the concrete elements. This finding has new inspiration for material mechanics and structural analysis. However, a more accurate stress state cannot be clarified, particularly for the shear transfer on complex interfaces, which needs to be realised by finite element simulation in future research. The method of strengthening the FRCM overlays by mechanical anchors assembly by bolt, nut, and washer on the RC frame, exemplified by Sagar et al., (2019), is also worth studying. In addition, only structural analysis was performed in this study.

Acknowledgements
For the research work of this paper, the author would like to express his sincere appreciation to Prof. Christis Chrysostomou and Prof. Nicholas Kyriakides for authorizing and sharing the original test data, Dr Renos Votsis for managing the project, Dr Rogiros Illampas for copying and sorting the data, Dr Christiana Filippou for reporting the tests, Dr Elpida Georgiou for providing

academic assistance, and the Cyprus Association of Civil Engineers (CYACE) for providing technical support during the tests.

Author contributions
FW declares that his contribution to this Research Article is 100%. The author read and approved the final manuscript. The authors read and approved the final manuscript.

Funding
The author declares that he did not receive any funding for creating this manuscript. The views and conclusions expressed in this article are solely those of the author and do not represent the views of any institution or organization. The original test data used in this research article were shared and generated from a project [name: SupERB-Novel integrated approach for seismic and energy upgrading of existing buildings (INTEGRATED/0916/0004)], which was co-funded by the European Regional Development Fund (ERDF) and Republic of Cyprus through the Research and Innovation Foundation (RIF).

Availability of data and materials
The data that support the conclusions of this study are available from the Cyprus University of Technology, but restrictions apply to the availability of these data, which were used under license for the current study, and so are not publicly available. Data are, however, available from the author upon reasonable request and with the permission of the Cyprus University of Technology.

Declarations

Competing interests
The author declares that he receives no financial or external non-financial support. FW was employed as a Research Fellow by the Cyprus University of Technology (CUT) from January 2nd, 2019 to December 2nd, 2021. He undertakes to ensure that his personal conduct is in accordance with the 'Inventions and Proprietary Information Agreement for CUT Employees and Students' and to report appropriately when there is a potential for actual or potential conflict.

Received: 10 January 2023 Accepted: 1 March 2023
Published: 29 May 2023

References

Abu Obaida, F., El-Maaddawy, T., & El-Hassan, H. (2021). Bond behavior of carbon fabric-reinforced matrix composites: geopolymeric matrix versus cementitious mortar. *Buildings, 11*(5), 16. https://doi.org/10.3390/buildings11050207

Akhoundi, F., Vasconcelos, G., Lourenço, P., Silva, L. M., Cunha, F., & Fangueiro, R. (2018). In-plane behavior of cavity masonry infills and strengthening with textile reinforced mortar. *Engineering Structures, 156*, 145–160. https://doi.org/10.1016/j.engstruct.2017.11.002

Alrshoudi, F. (2021). Textile-reinforced concrete versus steel-reinforced concrete in flexural performance of full-scale concrete beams. *Crystals, 11*(11), 20.

Al-Salloum, Y. A., Siddiqui, N. A., Elsanadedy, H. M., Abadel, A. A., & Aqel, M. A. (2011). Textile-reinforced mortar versus FRP as strengthening material for seismically deficient RC beam-column joints. *Journal of Composites for Construction, 15*(6), 920–933. https://doi.org/10.1061/(asce)cc.1943-5614.0000222

Bournas, D. A., Triantafillou, T. C., Zygouris, K., & Stavropoulos, F. (2009). Textile-reinforced mortar versus FRP jacketing in seismic retrofitting of RC columns with continuous or lap-spliced deformed bars. *Journal of Composites for Construction, 13*(5), 360–371. https://doi.org/10.1061/(asce)cc.1943-5614.0000028

Cerniauskas, G., Tetta, Z., Bournas, D. A., & Bisby, L. A. (2020). Concrete confinement with TRM versus FRP jackets at elevated temperatures. *Materials and Structures, 53*(3), 14. https://doi.org/10.1617/s11527-020-01492-x

Colajanni, P., Fossetti, M., & Macaluso, G. (2014). Effects of confinement level, cross-section shape and corner radius on the cyclic behavior of CFRCM confined concrete columns. *Construction and Building Materials, 55*, 379–389. https://doi.org/10.1016/j.conbuildmat.2014.01.035

Faleschini, F., Gonzalez-Libreros, J., Zanini, M. A., Hofer, L., Sneed, L., & Pellegrino, C. (2019). Repair of severely-damaged RC exterior beam-column joints with FRP and FRCM composites. *Composite Structures, 207*, 352–363. https://doi.org/10.1016/j.compstruct.2018.09.059

Illampas, R., Rigopoulos, I., & Ioannou, I. (2021). Influence of microencapsulated phase change materials (PCMs) on the properties of polymer modified cementitious repair mortar. *Journal of Building Engineering, 40*, 16. https://doi.org/10.1016/j.jobe.2021.102328

Ismail, N., El-Maaddawy, T., & Khattak, N. (2018). Quasi-static in-plane testing of FRCM strengthened non-ductile reinforced concrete frames with masonry infills. *Construction and Building Materials, 186*, 1286–1298. https://doi.org/10.1016/j.conbuildmat.2018.07.230

Karlos, K., Tsantilis, A., & Triantafillou, T. (2020). Integrated seismic and energy retrofitting system for masonry walls using textile-reinforced mortars combined with thermal insulation: experimental, analytical, and numerical study. *Journal of Composites Science, 4*(4), 16. https://doi.org/10.3390/jcs4040189

Morandi, P., Hak, S., & Magenes, G. (2018). Performance-based interpretation of in-plane cyclic tests on RC frames with strong masonry infills. *Engineering Structures, 156*, 503–521. https://doi.org/10.1016/j.engstruct.2017.11.058

Ngo, D. Q., Nguyen, H. C., Mai, D. L., & Vu, V. H. (2020). Experimental and numerical evaluation of concentrically loaded RC columns strengthening by textile reinforced concrete jacketing. *Civil Engineering Journal, 6*(8), 1428–1442. https://doi.org/10.28991/cej-2020-03091558

Papanicolaou, C. G., Triantafillou, T. C., Karlos, K., & Papathanasiou, M. (2006). Textile-reinforced mortar (TRM) versus FRP as strengthening material of URM walls: in-plane cyclic loading. *Materials and Structures, 40*(10), 1081–1097. https://doi.org/10.1617/s11527-006-9207-8

Papanicolaou, C. G., Triantafillou, T. C., Papathanasiou, M., & Karlos, K. (2007). Textile reinforced mortar (TRM) versus FRP as strengthening material of URM walls: out-of-plane cyclic loading. *Materials and Structures, 41*(1), 143–157. https://doi.org/10.1617/s11527-007-9226-0

Raoof, S. M., & Bournas, D. A. (2017a). Bond between TRM versus FRP composites and concrete at high temperatures. *Composites Part B: Engineering, 127*, 150–165. https://doi.org/10.1016/j.compositesb.2017.05.064

Raoof, S. M., & Bournas, D. A. (2017b). TRM versus FRP in flexural strengthening of RC beams: Behaviour at high temperatures. *Construction and Building Materials, 154*, 424–437. https://doi.org/10.1016/j.conbuildmat.2017.07.195

Raoof, S. M., Koutas, L. N., & Bournas, D. A. (2017). Textile-reinforced mortar (TRM) versus fibre-reinforced polymers (FRP) in flexural strengthening of RC beams. *Construction and Building Materials, 151*, 279–291. https://doi.org/10.1016/j.conbuildmat.2017.05.023

Ricci, P., Di Domenico, M., & Verderame, G. M. (2018). Experimental assessment of the in-plane/out-of-plane interaction in unreinforced masonry infill walls. *Engineering Structures, 173*, 960–978. https://doi.org/10.1016/j.engstruct.2018.07.033

Sagar, S. L., Singhal, V., & Rai, D. C. (2019). In-Plane and out-of-plane behavior of masonry-infilled RC frames strengthened with fabric-reinforced cementitious matrix. *Journal of Composites for Construction, 23*(1), 14. https://doi.org/10.1061/(asce)cc.1943-5614.0000905

Shi-ping, Y., Shi-chang, L., Xun, S., & Xiang-qian, H. (2020). Study of the mechanical properties of TRC-strengthened eccentric columns exposed to dry and wet cycles in a chloride salt erosion environment. *Engineering Structures, 204*, 12. https://doi.org/10.1016/j.engstruct.2019.110014

Singh, S. B., & Munjal, P. (2020). Engineered cementitious composite and its applications. *Materials Today: Proceedings, 32*, 797–802.

Su, Q. W., Cai, G. C., & Cai, H. R. (2017). Seismic behaviour of full-scale hollow bricks-infilled RC frames under cyclic loads. *Bulletin of Earthquake Engineering, 15*(7), 2981–3012. https://doi.org/10.1016/j.matpr.2020.03.743

Tetta, Z. C., Koutas, L. N., & Bournas, D. A. (2015). Textile-reinforced mortar (TRM) versus fiber-reinforced polymers (FRP) in shear strengthening of concrete beams. *Composites Part B: Engineering, 77*, 338–348. https://doi.org/10.1016/j.compositesb.2015.03.055

Toska, K., Faleschini, F., Zanini, M. A., Hofer, L., & Pellegrino, C. (2021). Repair of severely damaged RC columns through FRCM composites. *Construction and Building Materials, 273*, 13. https://doi.org/10.1016/j.conbuildmat.2020.121739

Trapko, T. (2014). Effect of eccentric compression loading on the strains of FRCM confined concrete columns. *Construction and Building Materials, 61*, 97–105. https://doi.org/10.1016/j.conbuildmat.2014.03.007

Trapko, T., & Musial, M. (2020). Effect of PBO-FRCM reinforcement on stiffness of eccentrically compressed reinforced concrete columns. *Materials, 13*(5), 17. https://doi.org/10.3390/ma13051221

Triantafillou, T. C., Karlos, K., Kefalou, K., & Argyropoulou, E. (2017). An innovative structural and energy retrofitting system for URM walls using textile reinforced mortars combined with thermal insulation: mechanical and fire behavior. *Construction and Building Materials, 133*, 1–13. https://doi.org/10.1016/j.conbuildmat.2016.12.032

Wang, F. Y., Kyriakides, N., Chrysostomou, C., Eleftheriou, E., Votsis, R., & Illampas, R. (2021). Experimental research on bond behaviour of fabric reinforced cementitious matrix composites for retrofitting masonry walls. *International Journal of Concrete Structures and Materials, 15*(1), 17. https://doi.org/10.1186/s40069-021-00460-1

Yan, Y., Liang, H., Lu, Y., & Zhao, X. (2021). Slender CFST columns strengthened with textile-reinforced engineered cementitious composites under axial compression. *Engineering Structures, 241*, 16. https://doi.org/10.1016/j.engstruct.2021.112483

Yin, S.-P., Peng, C., & Jin, Z.-Y. (2017). Research on mechanical properties of axial-compressive concrete columns strengthened with TRC under a conventional and chloride wet-dry cycle environment. *Journal of Composites for Construction, 21*(1), 11. https://doi.org/10.1061/(asce)cc.1943-5614.0000725

Publisher's Note

Fayu Wang Former Research Fellow at Department of Civil Engineering and Geomatics, Faculty of Engineering and Technology, Cyprus University of Technology; proposed Postdoctoral Researcher at Beijing Key Laboratory of Earthquake Engineering and Structural Retrofit, Beijing University of Technology.